Capsule-areal-density asymmetries inferred from 14.7-MeV deuterium–helium protons in direct-drive OMEGA implosions[a)]

C. K. Li,[b)] F. H. Séguin, J. A. Frenje, R. D. Petrasso,[c)] R. Rygg, S. Kurebayashi, and B. Schwartz
Plasma Science and Fusion Center, Massachusetts Institute of Technology, Cambridge, Massachusetts 02139

R. L. Keck, J. A. Delettrez, J. M. Soures, P. W. McKenty, V. N. Goncharov,[d)] J. P. Knauer, F. J. Marshall, D. D. Meyerhofer,[e)] P. B. Radha, S. P. Regan, T. C. Sangster, W. Seka, and C. Stoeckl
Laboratory for Laser Energetics, University of Rochester, Rochester, New York 14623

(Received 11 November 2002; accepted 17 December 2002)

Capsule-areal-density (ρR) asymmetries are studied for direct-drive, spherical implosions on the OMEGA laser facility [T. R. Boehly *et al.*, Opt. Commun. **133**, 495 (1997)]. Measurements of copious 14.7-MeV protons generated from D^3He fusion reactions in the imploded capsules are used to determine ρR. As they pass through the plasma, these protons lose energy, and this energy loss reflects the areal density of the transited plasma. Up to 11 proton spectrometers simultaneously view D^3He implosions on OMEGA from different directions. While the burn-averaged and spatially averaged ρR for each implosion is typically between 50 and 75 mg/cm^2 for 20-μm plastic shells filled with 18 atm of D^3He gas, significant differences often exist between the individual spectra, and inferred ρR on a given shot (as large as $\sim\pm 40\%$ about the mean). A number of sources inherent in the direct-drive approach to capsule implosions can lead to these measured ρR asymmetries. For example, in some circumstances these asymmetries can be attributed to beam-to-beam energy imbalance when this imbalance is relatively large ($\sim$25% rms). However, for more uniform illumination the source of the asymmetries is still under investigation. © *2003 American Institute of Physics.* [DOI: 10.1063/1.1556602]

I. INTRODUCTION

Achieving high quality spherical implosions is a critical and fundamental requirement in inertial confinement fusion (ICF). To achieve high gain and, eventually, ignition, capsule implosions must be extremely symmetric with asymmetries less than a few percent.[1–6] Tremendous efforts have been made in current ICF research to reduce implosion asymmetries by reducing target illumination nonuniformity and capsule imperfections. Characterization of the success of these efforts requires measurements of any deviations from spherical symmetry in the assembled capsule mass, or areal density (ρR—the product of the density and radius). Quantitative experimental information about asymmetries in ρR has not been available, however, until recent experiments[7] that used novel charged-particle spectrometry[8,9] to study direct-drive implosions at the OMEGA laser facility.[10,11] Previous work relied on numerical simulations to predict the conditions under which asymmetries may develop, and x-ray imaging to provide information about emission symmetry.[12–14] In this paper, we report recent charged-particle data on asymmetry, discuss results, and summarize our current understanding in the context of direct-drive implosions.

In the direct-drive approach to ICF, spherical implosion occurs in response to a large number of high-power laser beams illuminating the surface of the target capsule.[1–3] Illumination nonuniformity, coupled with initial capsule imperfections, lead to distortions in the compressed capsule. Plasma instabilities would amplify these distortions during both the acceleration and deceleration phases of the implosion. Asymmetries in ρR result from both high-mode ($\ell > 10$) Rayleigh–Taylor (RT) instabilities and low-mode-number ($\ell \leqslant 10$) secular modes.[15–17] High-mode-number perturbations are primarily imprinted by nonuniformities within individual laser beams and subsequently couple with capsule imperfections. These perturbations grow exponentially in their earlier phase until reaching saturation when their amplitudes are larger than $4R/\ell^2$ (R is the capsule radius); then they grow linearly.[18,19] The low-mode-number ρR asymmetries ($\ell \leqslant 10$) grow secularly and result primarily from drive pressure asymmetry due to nonuniformity in either initial capsule structure or laser intensity on target (power imbalance).[15–17,20]

Nonuniformities in the on-target laser intensity that cause drive pressure asymmetry occur due to a number of physical mechanisms including beam-to-beam power imbalance, beam mispointing and mistiming, imbalance of beam sizes and profiles, target-center offset, etc. Although the effects of lateral energy flow in the form of transverse thermal conduction help to reduce high-mode nonuniformities, they are negligible for low-mode perturbations ($\ell \leqslant 6$) for the ex-

[a)]Paper RI1 5, Bull. Am. Phys. Soc. **47**, 284 (2002).
[b)]Invited speaker.
[c)]Also Visiting Senior Scientist at LLE, University of Rochester.
[d)]Also Department of Mechanical Engineering, University of Rochester.
[e)]Also Department of Mechanical Engineering and Physics and Astronomy, University of Rochester.

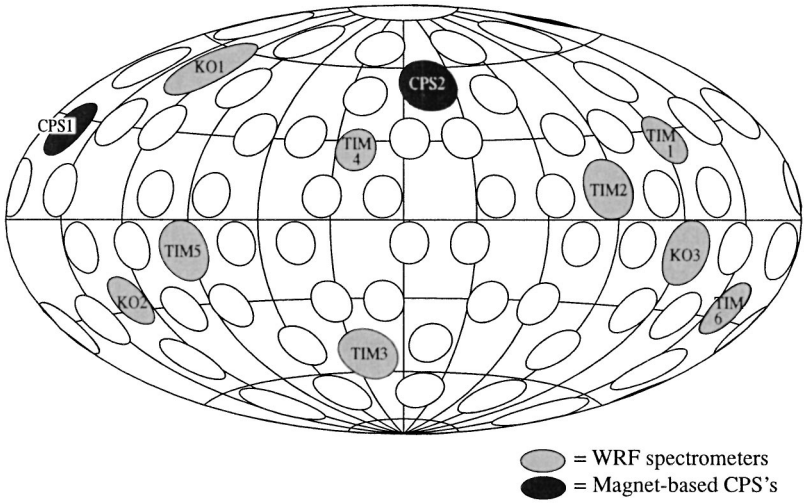

FIG. 1. Up to 11 diagnostic ports can be used for charged-particle spectroscopy on the OMEGA target chamber. Two of them are permanently mounted, magnet-based spectrometers CPS1 and CPS2. The others can be used for wedged-range-filter proton spectrometers (WRF's).

periments discussed here. This is because the separation between the critical surface and the ablation surface, typically $\sim 130\ \mu$m, is shorter than the scale length of low-mode nonuniformities (for example, $\sim 167\ \mu$m for $\ell \sim 6$). The laser-intensity nonuniformity should imprint itself on the target and result in variations in ablation pressure that are of the same order of variations in the laser intensity ($\delta P/P \sim \delta I/I$, where P is the ablation pressure and I is laser intensity).

On the OMEGA laser facility, significant improvements have been achieved for both the capsule quality and laser conditions. To reduce the effects of laser imprinting on target, beam-smoothing techniques have been applied to individual beams, including two-dimensional, single-color-cycle, 1-THz smoothing by spectral dispersion (2-D SSD) with polarization smoothing (PS) using birefringent wedges, and distributed-phase plates (DPP's), etc.[15–17,20] Recent experiments show that single-beam nonuniformities have been significantly reduced,[15–17,20] resulting in better capsule performance, presumably as a consequence of reduced RT seeding and reduced fuel-shell mix.[16,17,21,22] To reduce low-mode illumination asymmetry, the overlap of the 60 individual beams is carefully designed.[10,11] In current direct-drive experiments on OMEGA, laser conditions are typically characterized by the following parameters: laser power imbalance (same order as energy imbalance) $\sim 5\%$ rms or less; capsule target center offset $\leqslant 5\ \mu$m; beam mispointing $\leqslant 15\ \mu$m; mistiming <10 ps ($\sim 1\%$ of the laser duration); and nonuniformity of beam size and profile (effects of DPP distribution) $\sim 1.1\%$ rms for a 1-ns square pulse with 60 beams.[23] Improvements in all of these parameters have resulted in significant improvements in capsule implosion performance, including ρR symmetry.

The following sections discuss: (1) the analysis of OMEGA experiments, together with a description of how D^3He proton spectra are used to study ρR and ρR asymmetries; (2) experimental asymmetry data; (3) interpretation of their significance; and (4) the summary of the major results.

II. EXPERIMENTS AND ρR SYMMETRY MEASUREMENT METHODS

The experiments reported here used 60 beams of frequency-tripled (351-nm), UV light to directly drive the targets. OMEGA[10,11] delivers 60, symmetrically arranged beams with up to 30 kJ in 1 to 3 ns with a variety of pulse shapes. In this study, the laser energies were ~ 23 kJ, with a typical intensity of $\sim 1\times 10^{15}$ W/cm^2, and the laser-beam spot size on target was ~ 1 mm. The 1-ns square laser pulses had rise and decay times of $\leqslant 150$ ps. Good pulse-shape repeatability was obtained, and the beam-to-beam laser energy imbalance was typically $\sim 5\%$ rms. The individual beams were smoothed using single-color-cycle 2-D SSD, with 1.0-THz bandwidth, and polarization smoothing (PS) using birefringent wedges. Targets were room-temperature capsules with D^3He gas enclosed in plastic (CH) shells. Two gas-fill pressures (18 atm and 4 atm) were used, and all nominally had equal-atom amounts of deuterium and helium. The nominal CH-shell thickness was 20 μm, and the capsule diameters were $\sim 940\ \mu$m.

To study ρR asymmetry we measured multiple spectra of D^3He protons from the reaction

$$D + {}^3He \rightarrow \alpha(3.6\ \text{MeV}) + p(14.7\ \text{MeV}). \quad (1)$$

The 14.7-MeV protons are energetic enough to easily penetrate the CH shell of compressed capsules described here without having their spectral shape significantly distorted, but they interact strongly enough with the capsule plasma on their way out to make an accurate measurement of energy loss possible for probing of capsule compression (at the burn time). Charged-particle measurements provide the most sensitive diagnostic to date for detecting changes in ρR asymmetry.

On OMEGA, up to 11 charged-particle spectrometers can be used simultaneously to measure particles from different directions, as illustrated in Fig. 1. Two magnet-based charged-particle spectrometers (CPS1 and CPS2) and several wedged-range-filter spectrometers (WRF's) were used in this study.[8,9] For the CPS's, the energy calibration uncertainty

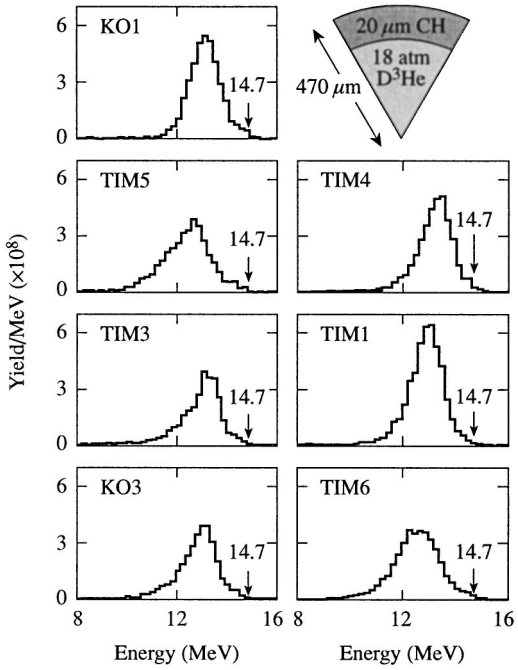

FIG. 2. Proton spectra measured simultaneously at seven different diagnostic ports (see Fig. 1 for port locations) for shot 25209 (20-μm CH shell filled with 18 atm of D^3He gas). Substantial asymmetries are clearly seen in the mean downshifted energy and the spectral end-point energy. The arrows show the proton's birth energies.

varies with particle energy, about 30 keV at 2 MeV and about 100 keV at 15 MeV. For WRF's, the current energy calibration is accurate to about 0.15 MeV at 15 MeV. Because the WRF's are simple and compact, they can be used at multiple positions during a shot for symmetry studies; they can also be placed close to the target for good statistics when proton yields are low (down to about 5×10^5).[9] Because a finite number of spectrometers can be used simultaneously and each spectrometer samples a significant angular fraction of a capsule's surface, only low-mode-number perturbations ($\ell \leqslant 5$) are detected sensitively.[7]

Figure 2 illustrates a sample set of seven proton spectra from a single implosion. The protons have known birth spectra (with mean energy $\langle E_0\rangle = 14.7$ MeV), and as they pass out of a capsule, they lose energy in proportion to the amount of material they pass through (ρR). Because the effects of capsule charging and particle acceleration are negligible in the experiments discussed here,[24,25] a value of ρR for the portion of a capsule facing a given spectrometer can be estimated from the downshift in mean proton energy ($\Delta\langle E_p\rangle = 14.7\ \text{MeV} - \langle E_p\rangle$) by using an appropriate theoretical formulation for the slowing down of protons in a plasma:

$$\rho R = \int_E^{E_0} \rho \left(\frac{dE}{dx}\right)^{-1} dE, \tag{2}$$

where (dE/dx) is the charged-particle stopping power in the plasma. Because of the relative high temperature and low density of the compressed core, D^3He protons lose their energies primarily in the CH shell, which has lower temperature but higher density than the core region where the nuclear reactions occur. Consequently, the inferred total ρR

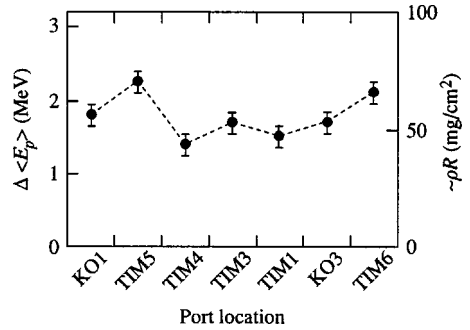

FIG. 3. Variations of the measured mean energy loss ($\Delta\langle E_p\rangle$) and corresponding ρR plotted versus port positions for the spectra displayed in Fig. 2 (shot 25209, see Fig. 1 for port locations). The error bars are instrumentation uncertainty ($\leqslant \pm 150$ keV), which are much smaller than the measured ρR asymmetries.

is approximately the shell ρR and the measured total ρR asymmetries largely reflect shell ρR asymmetries. In addition, because D^3He protons are so energetic, the calculation is relatively insensitive to uncertainties in the temperature and density of the CH shell.[24]

The variations of the measured $\Delta\langle E_p\rangle$ and corresponding ρR are plotted versus measurement port location (Fig. 3) for the spectra shown in Fig. 2. The average mean energy loss was $\Delta\langle E_p\rangle \sim 1.8$ MeV, and substantial energy loss asymmetries are clearly seen. Variations about the mean are as large as ± 0.4 MeV. Since spectrometer-to-spectrometer differences in $\Delta\langle E_p\rangle$ are sensitive only to low-mode-number structure, the variation indicates the presence of low-mode-number ρR asymmetries.

III. ASYMMETRY MEASUREMENTS FOR DIFFERENT SHOT PARAMETERS

In this section, measurements of D^3He proton energy spectra are used to illustrate ρR asymmetries and their relationship to some experiment parameters. Interpretation of the asymmetries will be discussed in Sec. IV. We begin with data from shots involving capsules with different D^3He-fill pressures and shots made during different time intervals, shown in Figs. 4–6. Specifically, plotted in Fig. 4, $\Delta\langle E_p\rangle$ and inferred ρR are compared for two shots, similar except for very different gas-fill pressures (4 and 18 atm, see Fig. 1 for

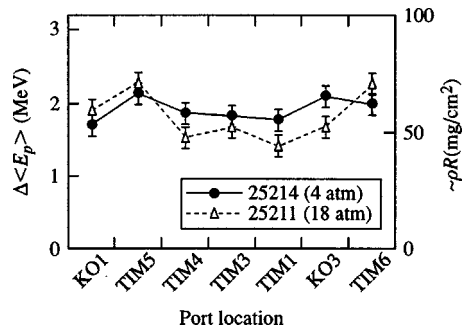

FIG. 4. $\Delta\langle E_p\rangle$ and inferred ρR are compared for two shots, similar except for very different gas-fill pressures (4 and 18 atm, see Fig. 1 for port locations). Despite this difference, the deviations from spherical symmetry are similar.

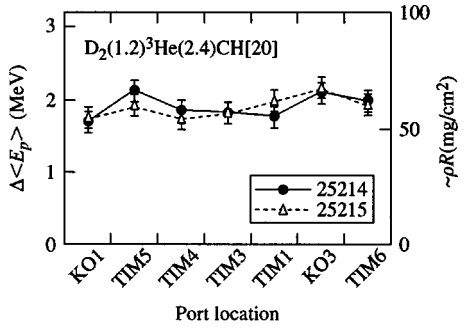

FIG. 5. $\Delta\langle E_p\rangle$ and inferred ρR for two sequential implosions, both with 4 atm of D^3He. As shown here, the asymmetries of contiguous shots are often quite similar.

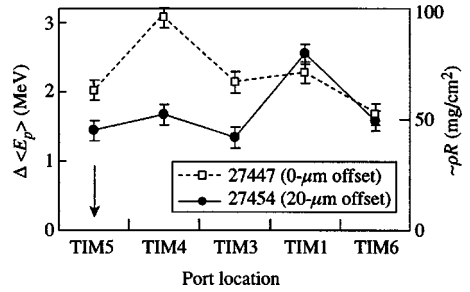

FIG. 7. $\Delta\langle E_p\rangle$ and inferred ρR measured at different port locations for two OMEGA implosions: one with a target offset of 20 μm toward the direction of port TIM5 (arrow) and the other with zero offset (see Fig. 1 for port locations). The fact that variations due to the 20-μm-offset shot are no larger than those measured with zero offset suggests that at this level, offsets alone cannot be responsible for the measured asymmetries.

port locations). Despite this difference, the deviations from spherical symmetry are similar. Figure 5 shows $\Delta\langle E_p\rangle$ and inferred ρR for two sequential implosions, both with 4 atm of D^3He. As shown here, the asymmetries of contiguous shots are often quite similar. Figure 6 shows representative $\Delta\langle E_p\rangle$ (and corresponding ρR) for three shot sequences during one day: (a) morning, (b) afternoon, and (c) evening (see Fig. 1 for port locations). The laser conditions and capsules were nominally the same except for fill pressure, a parameter for which there is, at most, a weak dependence (see Fig. 10).

Apart from the low-mode structure apparent in Figs. 4–6, which will be discussed below, it is apparent from the mean values of $\Delta\langle E_p\rangle$ (and inferred ρR) that total capsule compression is quite insensitive to fill pressure. This result is consistent with ρR measurements made previously using knock-on protons from implosions of CH-shell capsules with DT-gas fill; similar shell ρR values were also obtained for different gas-fill pressures.[22] These results are in contrast with one-dimensional (1-D) calculations,[26] which predict that implosions with lower fill pressure capsules should result in much higher shell compressions. The consistency of the results obtained with two entirely different methods and different capsule types makes the experimental conclusion unequivocal. The possibility that the spectrometers are somehow artificially limited to values of ρR below those predicted for the low fill pressures can be ruled out because values as high as $\sim$100 mg/cm^2 have been measured for picket-pulse capsule implosions.[27] The physics behind the discrepancy between experiments and 1-D simulations, as discussed in detail elsewhere,[22] is likely to involve the effects of fuel-shell mix (which is not included in 1-D calculations). Capsules with low gas pressure are more unstable to the Rayleigh–Taylor instability. During the deceleration phase of an implosion, distortions at the fuel-shell interface grow and result in the mixing of the fuel and shell materials. This kind of mix would degrade target implosion performance, including the reduction of the capsule compressions. It has been demonstrated[22] for D_2 and DT shots that unstable capsules (lower gas-fill pressure or thinner shell) result in compression falling short of 1-D prediction while relatively stable capsules would result in implosions close to 1-D predictions.

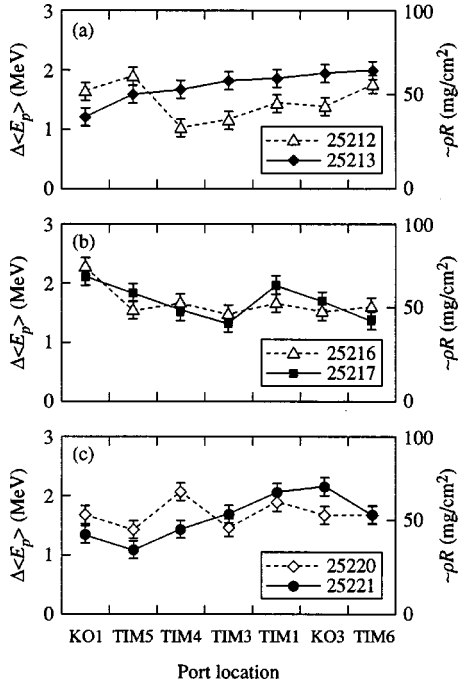

FIG. 6. Representative $\Delta\langle E_p\rangle$ (and corresponding ρR) for three shot sequences during one day: (a) morning, (b) afternoon, and (c) evening (see Fig. 1 for port locations). The laser conditions and capsules were nominally the same except for fill pressure, a parameter for which there is, at most, a weak dependence (see Fig. 10).

The effects of target offset on the measured ρR asymmetry are illustrated in Fig. 7. The data shown correspond to the conditions of zero offset and 20 μm of offset (toward TIM5, or port H14). These two offsets were chosen because, under current OMEGA operation, the uncertainty in the target-center offset is $\leqslant$5 μm for room-temperature capsules.

IV. PRELIMINARY DISCUSSION OF POSSIBLE SOURCES OF THE ρR ASYMMETRIES

Completely addressing the issue of possible sources of the measured low-mode-number ρR asymmetries is a significant undertaking. In this section we discuss some of the possible effects of individual sources in light of the data shown above. To understand ρR asymmetries for direct-drive implosions on OMEGA, a number of mechanisms should be considered, including initial capsule structure asymmetries,

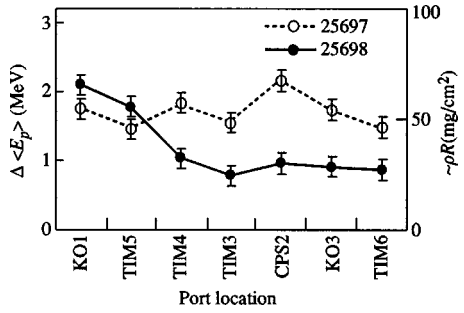

FIG. 8. Proton energy downshifts measured at seven different port locations for two contiguous shots. For shot 25698 (the imbalance is ~24.2% rms), the measured ρR asymmetries are strongly correlated with the beam-energy imbalance, where both the laser imbalance and asymmetry are dominated by an $\ell \sim 1$ mode.

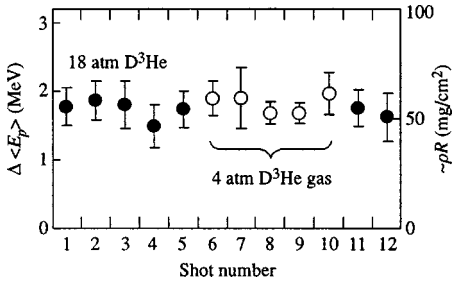

FIG. 10. $\Delta\langle E_p\rangle$ and ρR measured for the different shots recorded during the same day (some of the data are illustrated in Fig. 6). Values are averaged over a maximum of seven port locations. Variations of these measurements for each individual shot are characterized with a standard deviation, reflecting the ρR asymmetries and their range.

offset of the target chamber center (TCC), beam mispointing and mistiming, the effects of DPP on the beam size and profiles, power imbalance, etc.

The measured ρR asymmetries appear to have completely different features for energy imbalance within the regimes of ~5% rms and ~25% rms, as shown by the two contiguous shots in Fig. 8. Shot 25697, for which the energy imbalance is ~6.4% rms, displays a distributed ρR asymmetry with a small amplitude of variations (±20% to its mean), while shot 25698, for which the energy imbalance is ~24.2% rms, displays a strong ρR asymmetry in several particular directions (a factor of 2 smaller than the other directions with normal illumination). These are strongly correlated with energy imbalance. Specifically, for this shot the total laser energy is ~21 kJ with $\langle E_{\mathrm{UV}}\rangle \approx 350.6$ J/beam. Because four laser beams (beam 32, 37, 62, and 67) dropped out (only delivered ~10% to 15% of $\langle E_{\mathrm{UV}}\rangle$) during the laser illuminations, a strong nonuniformity of laser intensity ($\sigma_{\mathrm{rms}} \sim 9\%$) was imposed on the target, with a dominant $\ell \sim 1$ mode as illustrated in Fig. 9. Because of the beam overlapping on the target surface, the intensities on the spots of these beams are ~70% to 80% of the mean irradiance. This asymmetry of energy deposited directly causes ablation pressure asymmetry and, consequently, results in ρR asymmetry. Among the seven spectrometers used for this shot, five (port TIM4, TIM3, CPS2, KO3, and TIM6) were pointed towards the spots of these four beams while KO1 and TIM5 viewed the nominal intensity region: The lower laser intensity leads to lower ρR in these directions. This clearly demonstrates that in this case the measured ρR asymmetries are correlated primarily with the beam-energy imbalance.

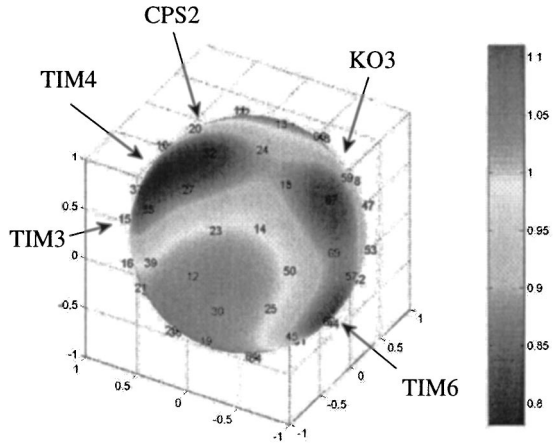

FIG. 9. The calculated on-target laser-intensity distribution for shot 25698 shows a strong $\ell \sim 1$ asymmetry. The five ports (TIM3, TIM4 CPS2, KO3 and TIM6) centered about beams 32, 37, 62, and 67, indicated in the figure, were directed toward this region of low laser intensity.

The issue of target offset with respect to target chamber center is related to laser-beam balance because a change in the target position results in a change in the spatial distribution of on-target laser intensity, even if the beams themselves do not move. It can be seen from Fig. 7 that a 20-μm offset does not induce asymmetries any larger than those seen in the similar shot with no offset. This implies that the offset may be a factor but is not the only source of ρR asymmetry, under these conditions.

Although we have seen that shots close to each other in time are often very similar, there often tends to be a drift in asymmetry structure over time scales comparable to a day or more, as illustrated in Fig. 6. The cause for this is not currently clear; it may have something to do with a drift in the optics that could cause small changes in laser energy transmission efficiency.

Some indication of the variations seen within shots and over time can be obtained by looking at all of the data for one day (of which Fig. 6 showed a subset). Figure 10 shows the measured $\Delta\langle E_p\rangle$ and ρR averaged over all port locations for each individual shot and plotted versus shot number. Figure 11 shows measured $\Delta\langle E_p\rangle$ and inferred ρR (averaged over seven shots for 18 atm, and five shots for 4 atm) at the different port locations; variations in measurements at a given port are characterized by standard deviations about the mean. While Fig. 6 illustrates differences between the detailed asymmetry structures of different shots, Fig. 10 shows that the spatially averaged ρR for individual shots is relatively constant in time. Figure 11 shows that the time-averaged ρR value is relatively constant in space (at different measuring angles). The scatter indicated by the standard deviations shown in the figures is also roughly constant over time and space, indicating that the measured ρR asymmetry amplitudes are relatively repeatable even while the details of the structure become uncorrelated over time.

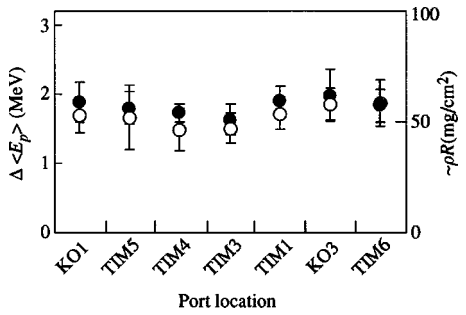

FIG. 11. $\Delta\langle E_p\rangle$ and inferred ρR [averaged over seven shots for 18 atm (open circles), and five shots for 4 atm (solid circles)] are plotted versus measurement port location. Each measurement is characterized with a standard deviation, reflecting the ρR variations.

V. CONCLUSIONS

Using charged-particle spectrometry, we have studied capsule-areal-density asymmetries for direct-drive, spherical implosions on OMEGA. Measurements of 14.7-MeV protons generated from D^3He fusion reactions in the imploded capsules provide unique evidence of the existence of the low-mode-number ρR asymmetries in imploded capsules. While the burn-averaged and spatially averaged ρR for each implosion is typically between 50 and 75 mg/cm^2 within a group of similar implosions, significant differences often exist between the individual ρR values inferred from spectrometers at different angles with respect to the capsule (as large as $\sim\pm 40\%$ about the mean). Under current OMEGA experimental conditions, the source of the measured asymmetries is still under investigation, but improvement in on-target laser uniformity planned for the near future, may both reduce the asymmetries and shed light on their origin.

ACKNOWLEDGMENTS

This work was performed in part at the LLE National Laser Users' Facility (NLUF), and was supported in part by the U.S. Department of Energy Contract No. DE-FG03-99SF21782, LLE subcontract No. PO410025G, LLNL subcontract No. B313975, the U.S. Department of Energy Office of Inertial Confinement Fusion under Cooperative Agreement No. DE-FC03-92SF19460, and the New York State Energy Research and Development Authority.

[1] S. W. Haan, S. M. Pollaine, J. D. Lindl *et al.*, Phys. Plasmas **2**, 2480 (1995).
[2] J. D. Lindl, *Inertial Confinement Fusion: The Quest for Ignition and Energy Gain Using Indirect Drive* (Springer-Verlag, New York, 1998).
[3] J. D. Lindl, R. L. McCrory, and E. M. Campbell, Phys. Today **45** (9), 32 (1992).
[4] J. H. Gardner and S. E. Bodner, Phys. Rev. Lett. **47**, 1137 (1981).
[5] M. H. Emery, J. H. Orens, J. H. Gardner, and J. P. Boris, Phys. Rev. Lett. **48**, 253 (1982).
[6] R. D. Petrasso, C. K. Li, M. D. Cable *et al.*, Phys. Rev. Lett. **77**, 2718 (1996).
[7] F. H. Séguin, C. K. Li, J. A. Frenje *et al.*, Phys. Plasmas **9**, 3558 (2002).
[8] D. G. Hicks, Ph.D. thesis, Massachusetts Institute of Technology, 1999.
[9] F. H. Séguin, J. A. Frenje, C. K. Li *et al.*, Rev. Sci. Instrum. **74**, 975 (2003).
[10] J. M. Soures, R. L. McCrory, C. P. Verdon *et al.*, Phys. Plasmas **3**, 2108 (1996).
[11] T. R. Boehly, D. L. Brown, R. S. Craxton *et al.*, Opt. Commun. **133**, 495 (1997).
[12] F. J. Marshall, J. A. Delettrez, R. L. Keck, J. H. Kelly, P. B. Radha, and L. J. Waxer, Bull. Am. Phys. Soc. **46**, 179 (2001).
[13] B. Yaakobi, V. A. Smalyuk, J. A. Delettrez *et al.*, Phys. Plasmas **7**, 3727 (2000).
[14] V. A. Smalyuk, B. Yaakobi, J. A. Delettrez, F. J. Marshall, and D. D. Meyerhofer, Phys. Plasmas **8**, 2872 (2001).
[15] S. Skupsky and R. S. Craxton, Phys. Plasmas **6**, 2157 (1999).
[16] R. L. McCrory, R. E. Bahr, R. Betti *et al.*, Nucl. Fusion **41**, 1413 (2001).
[17] D. D. Meyerhofer, J. A. Delettrez, R. Epstein *et al.*, Phys. Plasmas **8**, 2251 (2001).
[18] S. W. Haan, Phys. Rev. A **39**, 5812 (1989).
[19] T. R. Dittrich, B. A. Hammel, C. J. Keane, R. McEachern, R. E. Turner, S. W. Haan, and L. J. Suter, Phys. Rev. Lett. **73**, 2324 (1994).
[20] C. K. Li, F. H. Séguin, D. G. Hicks *et al.*, Phys. Plasmas **8**, 4902 (2001).
[21] P. B. Radha, J. A. Delettrez, R. Epstein *et al.*, Phys. Plasmas **9**, 2208 (2002).
[22] C. K. Li, F. H. Séguin, J. A. Frenje *et al.*, Phys. Rev. Lett. **89**, 165002 (2002).
[23] F. J. Marshall, P. W. McKenty, T. J. Kessler, R. Forties, J. A. Kelly, and L. Waxer, Bull. Am. Phys. Soc. **47**, 143 (2002).
[24] C. K. Li, D. G. Hicks, F. H. Séguin *et al.*, Phys. Plasmas **7**, 2578 (2000).
[25] D. G. Hicks, C. K. Li, F. H. Séguin *et al.*, Phys. Plasmas **7**, 5106 (2000).
[26] E. B. Goldman, Laboratory for Laser Energetics Report No. 16, University of Rochester, 1973.
[27] J. P. Knauer, V. N. Goncharov, P. W. McKenty *et al.*, "Improved performance of direct-drive implosions with a laser-shaped adiabat," Phys. Rev. Lett. (submitted).